Article

Facile Synthesis of β-Tetracyano Vanadyl Porphyrin from Its Tetrabromo Analogue and Its Excellent Catalytic Activity for Bromination and Epoxidation Reactions

Mannar R. Maurya,* Ved Prakash, Tawseef Ahmad Dar, and Muniappan Sankar*

Read Online

ACCESS | Metrics & More | Article Recommendations | SI Supporting Information

ABSTRACT: Complex 2,3,12,13-tetracyano-5,10,15,20-tetraphenylporphyrinatooxidovanadium(IV) $\{[V^{IV}OTPP(CN)_4], \mathbf{2}\}$ has been prepared by nucleophilic substitution of β-bromo groups of the corresponding 2,3,12,13-tetrabromo-5,10,15,20-tetraphenylporphyrinatooxidovanadium(IV) $\{[V^{IV}OTPP(Br)_4], \mathbf{1}\}$ using CuCN in quinoline. Both complexes show biomimetic catalytic activity similar to enzyme haloperoxidases and efficiently brominate various phenol derivatives in the presence of KBr, H_2O_2, and $HClO_4$ in the aqueous medium. Between these two complexes, **2** exhibits excellent catalytic activity with high turnover frequency ($35.5-43.3$ s^{-1}) due to the strong electron-withdrawing nature of the cyano groups attached at β-positions and its moderate nonplanar structure as compared to **1** (TOF = $22.1-27.4$ s^{-1}). Notably, this is the highest turnover frequency value observed for any porphyrin system. The selective epoxidation of various terminal alkenes using complex **2** has also been carried out, and the results are good, specifying the importance of electron-withdrawing cyano groups. Catalysts **1** and **2** are recyclable, and the catalytic activity proceeds through the corresponding $[V^VO(OH)TPP(Br)_4]$ and $[V^VO(OH)TPP(CN)_4]$ intermediates, respectively.
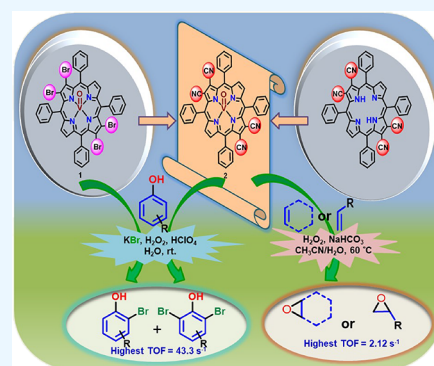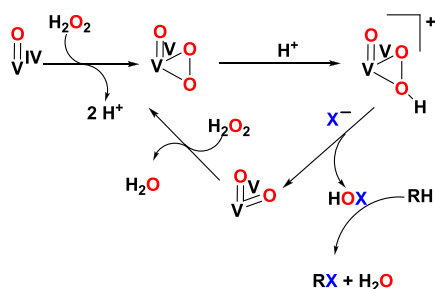
INTRODUCTION

Vanadium-dependent haloperoxidase (V-HPO) enzymes are known to play a key role in the oxidation of X^- (X^- = halide ions) in the presence of hydrogen peroxide.[1] During the oxidation of X^-, also observed in the functional model as well as in kinetics studies, the in situ generated oxido(peroxido)-vanadium(V) species allows nucleophilic attack of the halide ion, followed by the release of HOX/X_2, which actually halogenate the substrates (Scheme 1).[2−7]

Since oxidative halogenation occurs in the acidic medium, homogeneous functional models generally decompose at lower pH. Even metal complexes of unsubstituted porphyrins generally tend to undergo degradation[8] in oxidation- and oxidative bromination-type reactions, while complexes with β- and meso-functionalized porphyrins not only make them stable[9] toward degradation but also tune them to attain good thermal and chemical stabilities.[10,11] The high stability and recyclability of β- and meso-functionalized vanadyl porphyrins even at low pH (ca. 1.5)[12] are therefore suitable for developing new haloperoxidase mimetic catalysts. Furthermore, a highly electron-deficient porphyrin coordinated to the vanadyl center shows an excellent catalytic reaction due to an increase in the Lewis acidic nature of the complex.[12] Based on the biomimetic haloperoxidase reaction, recently, we developed a method for the self-catalyzed oxidative bromination of β-positions of the pyrrole ring of complex $[V^{IV}OTPP]$ in excellent yield under mild conditions without brominating the meso-phenyl rings.[12] Furthermore, the brominated $[V^{IV}OTPP(Br)_8]$ and $[V^{IV}OTPP]$ are highly active recyclable catalysts for the oxidative bromination of phenol derivatives.
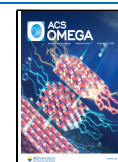
Scheme 1. Functional Model Considering the Oxidovanadium(IV) or Dioxidovanadium(V) Complex for the Generation of HOX and Subsequent Non-Catalytic Bromination

Scheme 2. Synthetic Route to Prepare Free-Base H$_2$TPP(CN)$_4$

H$_2$TPPBr$_4$ $\xrightarrow[\substack{\text{CHCl}_3/\text{MeOH,}\\\text{reflux}}]{\text{Ni(acetate)}_2}$ [Ni^{II}TPP(Br)$_4$] $\xrightarrow[\text{Reflux, 48 h}]{\text{CuCN, Pyridine}}$ [Ni^{II}TPP(CN)$_4$] $\xrightarrow[\text{(ii) NaHCO}_3]{\text{(i) H}_2\text{SO}_4}$ [H$_2$TPP(CN)$_4$]

85–90 %   56 %   85 %

Scheme 3. Synthetic Routes for 2 and Molecular Structure of Synthesized Oxidovanadium(IV) Complexes 1 and 2

Despite tremendous progress in synthetic organic chemistry over the past many years, bromination of phenol derivatives remains an area of focus owing to the use of its products in further reactions in industries as intermediates for fine chemicals and pharmaceuticals.[13,14] Porphyrins act as multifaceted ligands coordinating with various metals to form metalloporphyrins with many catalytic applications.[15−17] In living systems, porphyrins and their analogues perform many vital functions like oxygen transport and storage, photosynthesis, and electron transfer and as cofactors to many enzymes.[18−20] Porphyrins have also been found to possess remarkable applications in the fields of solar energy,[21] medicine,[22] sensing,[23] catalysis,[24] and nonlinear optics.[25]

Furthermore, we observed that all bromo groups of the vanadium(IV) complex of tetrabrominated β-positions of the pyrrole, i.e., 2,3,12,13-tetrabromo-5,10,15,20-tetraphenylporphyrinatooxidovanadium(IV) {[V^{IV}OTPP-(Br)$_4$], **1**}, can easily be cyanated to obtain 2,3,12,13-tetracyano-5,10,15,20-tetraphenylporphyrinatooxidovanadium-(IV) {[V^{IV}OTPP(CN)$_4$], **2**} in a single step under suitable reaction conditions. Therefore, we present herein two alternate methods for the synthesis of [V^{IV}OTPP(CN)$_4$], **2**: (i) a single-step direct cyanation of [V^{IV}OTPP(Br)$_4$], **1**, using CuCN in quinoline, and (ii) reaction of VOSO$_4$ with free-base H$_2$TPP-(CN)$_4$; the isolation of the free base is a multi-step process (Scheme 2).[26] The catalytic potential of both complexes (**1** and **2**) has been explored for the oxidative bromination of phenol derivatives. Complex **2** has also been utilized as a catalyst for selective epoxidation of olefins.

RESULTS AND DISCUSSION

Synthesis and Characterization of Complexes. Complex [V^{IV}OTPP(Br)$_4$] (**1**) can easily be prepared by reacting H$_2$TPPBr$_4$ with VOSO$_4$·xH$_2$O in refluxing DMF under an argon atmosphere.[27−29] Synthesis of [V^{IV}OTPP(CN)$_4$] (**2**) has been achieved by the direct cyanation of [V^{IV}OTPP(Br)$_4$] (**1**) via nucleophilic substitution with CuCN in quinolone under an argon atmosphere (Scheme 3) in a single step. This method has earlier been applied by some of us for the synthesis of [Cu^{II}TPP(CN)$_4$].[30] Alternatively, the reaction of free-base H$_2$TPP(CN)$_4$ with VOSO$_4$·xH$_2$O in DMF under reflux conditions for 30 h also gives **2**. However, isolation of free-base H$_2$TPP(CN)$_4$ itself is a tedious three-step process, as shown in Scheme 2. Moreover, the overall yield of **2** is about 23% compared to 29% from the first method. Therefore, the first method is much better and time saving.

UV−vis and IR Spectral Studies. The UV−vis spectrum of **1** in CH$_2$Cl$_2$ exhibits a single Soret band at 435 nm, which is almost similar to that of H$_2$TPPBr$_4$ (436 nm), and two Q bands (560 and 604 nm) compared to three in the case of H$_2$TPPBr$_4$ (533, 612, and 685 nm). Thus, the first Q band is 27 nm red-shifted while the second Q band is 8 nm blue-shifted relative to H$_2$TPPBr$_4$ upon metalation with the vanadium ion. Replacement of bromo groups at β-positions of the porphyrin ring by the cyano group of **1** caused the shifting of the Soret band to 442 nm in **2** (Figure 1), which is expected due to the more electron-

Figure 1. UV−vis spectra of [V^{IV}OTPP(Br)$_4$] (**1**) and [V^{IV}OTPP-(CN)$_4$] (**2**) in CH$_2$Cl$_2$ at 298 K.

withdrawing nature of the −CN group as compared to −Br. Similarly, the two Q bands also shifted to higher wavelengths by 17 and 21 nm, respectively, and appeared at 577 and 625 nm. Furthermore, the peak at 625 nm is relatively more intense in the case of **2** compared to the corresponding Q band of **1**. Two weak shoulder peaks arose at ca. 425 and 530 nm in **2**, which is possibly due to the charge transfer from the porphyrin ring to the −CN group (highly electron-withdrawing group). In the IR spectrum, characteristic peaks due to the ν(V=O) and ν(C−Br) stretches were located at 1010 and 619 cm^{-1} (Figure S1), respectively. The cyano groups present on the β-positions of the porphyrin ring caused the appearance of ν(V=O) at 1015 cm^{-1} in **2**, which is 5 cm^{-1} higher than that found in **1**. The absence of ν(C−Br) and the presence of the ν(C≡N) stretch at 2230 cm^{-1} (Figure S2) again validated the replacement of all bromo groups by CN.
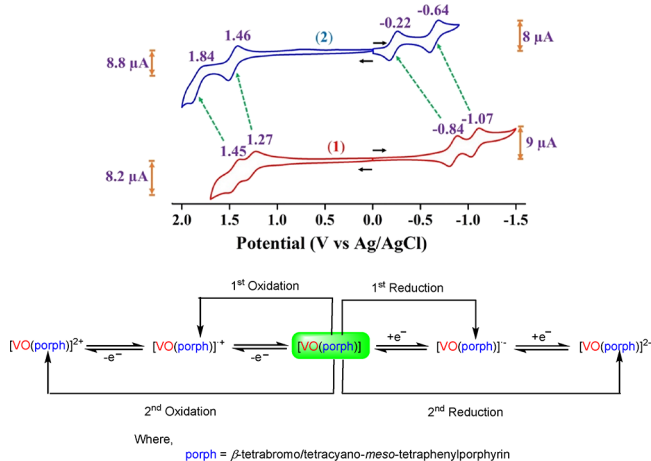
Mass Spectrometry and Thermogravimetric Study.
The found and calculated MALDI-TOF mass values for both complexes [1, m/z: found 995.99 [M]$^+$ (calcd. 995.24) and 2, m/z: found 779.53 [M]$^+$ (calcd. 779.15)] (Figures S3 and S4) are in good agreement and support the formation of expected complexes. As thermal stability has been considered one of the important parameters in terms of the catalytic suitability of complexes, the thermogravimetric profiles of these complexes were obtained. Both complexes are thermally stable (decomposition temperature: 230 °C for 1 and 275 °C for 2), and within these two, 2 is more stable than 1 (Figures S5 and S6), which may be attributed to the higher strength of C−C bonds (346 kJ/mol) and C≡N bonds (887 kJ/mol) relative to C−Br bonds (285 kJ/mol). Increasing the temperature further, both complexes decomposed exothermically in two overlapping steps. Complex 1 finally stabilized at 530 °C with a residue of 9.1%, while 2 stabilized at 430 °C with a residue of 10.5%. These values are close to the theoretical values of 9.04 and 11.68%, respectively, for V_2O_5.

Electrochemical Study. The electrochemical study of [V^{IV}OTPP] has been well explored in non-aqueous medium.[31] To understand the electrochemistry of synthesized complexes, we recorded a cyclic voltammogram of these compounds in distilled CH_2Cl_2 at 298 K using Ag/AgCl as the reference electrode and TBAPF$_6$ as the supporting electrolyte. The cyclic voltammogram of 1 exhibited two oxidation peaks at 1.27 and 1.45 V, while 2 displayed the corresponding oxidation peaks at 1.46 and 1.84 V, respectively. Similarly, two reduction peaks were obtained at −0.84 and −1.07 V in 1 and at −0.22 and −0.64 V in 2 (Figure 2). Table 1 provides all parameters. The

first and second oxidation potentials in the case of 2 are 0.19 and 0.39 V, anodically shifted compared to 1, whereas the first and second reduction potentials of 2 are 0.62 and 0.43 V, anodically shifted compared to 1. Therefore, cyclic voltammetry supports the more electron-deficient nature of 2 compare to 1.[31,32]

DFT Optimization Study. A DFT optimization study using the B3LYP functional and the LANL2DZ basis set was carried out for 1 and 2 in the gas phase. The optimized geometries of 1 and 2 are compared in Figure 3. Both 1 and 2 exhibited
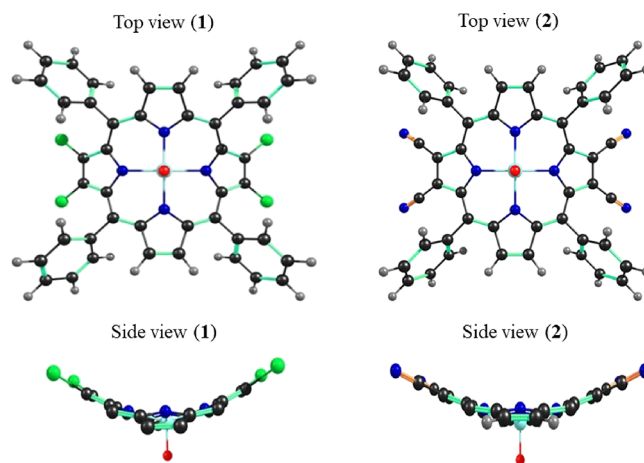
Figure 3. B3LYP/LANL2DZ set-optimized geometries of 1 and 2 in the gaseous phase showing top and side views (where β-hydrogens and *meso*-phenyl substituents have been removed for clarity).

nonplanar, saddle shape conformation, with 1 being relatively more distorted due to bulkier bromine atoms. In the case of 1, $\Delta24$ was found to be ±0.3829 Å while a similar value in the case of 2 was found to be ±0.2302 Å only. ΔC_β (carbon atoms having −Br or −CN substituents were taken as β) values were calculated to be ±0.8545 Å and ±0.538 Å for 1 and 2, respectively. Similarly, $\Delta C_{\beta'}$ (carbon atoms attached to −H atoms were taken as β') values for 1 and 2 were calculated to be ±0.725 and ±0.418 Å, respectively. Likewise, the Δ_M (M = metal) values in 1 and 2 were calculated to be 0.538 and 0.529 Å, respectively. Various bond distance values in 1 were calculated to be 1.593 Å (V=O), 1.379 Å (C_β−C_β), and 1.372 Å ($C_{\beta'}$−$C_{\beta'}$). The corresponding bond distances in 2 were found to be 1.591, 1.396, and 1.370 Å.

EPR Study. The X-band EPR spectra of [V^{IV}OTPP(Br)$_4$] (1) and [V^{IV}OTPP(CN)$_4$] (2) were recorded in toluene at 100 K (Figure 4). The spectra of both complexes exhibit similar eight lines, indicating the presence of vanadium metal ($I = 7/2$) at the porphyrin center in +4 oxidation state with one unpaired electron. The spin Hamiltonian parameters were obtained from the simulated EPR spectra of complexes 1 and 2, which are in close agreement with the corresponding experimentally observed spectrum. For complex 1, $g_\parallel$ and $g_\perp$ were found to be 1.9603 and 1.9825, respectively. The corresponding calculated values were 1.9603 and 1.9841, respectively. The $A_\parallel$ and $A_\perp$ values were found to be 159.6×10^{-4} and 56.0×10^{-4} cm^{-1}, respectively, while the calculated values were 159.2×10^{-4} and 56.6×10^{-4} cm^{-1}, respectively. Similarly, for 2, $g_\parallel$ and $g_\perp$ were found to be 1.9605 and 1.983 (calc.: 1.9605 and 1.9879), respectively, while $A_\parallel$ and $A_\perp$ values were found to be 160.2×10^{-4} and 57.2×10^{-4} cm^{-1} (calc.: 160.6×10^{-4}, 57.3×10^{-4} cm^{-1}), respectively. The $g_\parallel < g_\perp$ and $A_\parallel \gg A_\perp$ relationships are normal for the axially compressed d$^1_{xy}$ configuration;[33,34] thus,

Figure 2. Above: cyclic voltammograms of 1 and 2 in triple-distilled CH_2Cl_2 at 298 K using Ag/AgCl as the reference electrode and 0.1 M TBAPF$_6$ as the supporting electrolyte. Below: redox reactions of complexes 1 and 2.

Table 1. Electrochemical Redox Data[a] of 1 and 2 in CH_2Cl_2

	oxidation(V)		reduction(V)		
porphyrin[a]	II	I	I	II	ΔE (V)[b]
[V^{IV}OTPP(Br)$_4$], 1	1.45	1.27	−0.84	−1.07	2.11
[V^{IV}OTPP(CN)$_4$], 2	1.84	1.46	−0.22	−0.64	1.68

[a]vs. the Ag/AgCl reference electrode and the Pt working and Pt wire auxiliary electrodes. 0.1 M TBAPF$_6$ as the supporting electrolyte at 298 K. [b]$\Delta E = I_{oxidation} - I_{reduction}$.

Figure 4. X-band EPR spectra of $[V^{IV}OTPP(Br)_4]$ (**1**) and $[V^{IV}OTPP(CN)_4]$ (**2**) in toluene at 100 K (blue) and their corresponding simulated spectra (red). EPR parameter: microwave frequency, 9.388 GHz; incident microwave power, 0.717 mW.

Table 2. Oxidative Bromination of 4-Methylphenol (1.08 g, 10 mmol) Using $[V^{IV}OTPP(CN)_4]$ (2) as the Catalyst under Different Reaction Conditions

							% selectivity	
entry	catalyst (mg, μmol)	KBr (g, mmol)	H_2O_2 (g, mmol)	$HClO_4$ (g, mmol)	time (min)	% conversion	mono-bromo	di-bromo
1	0.20, 0.256	1.19, 10	1.13, 10	1.43, 10	120	70	100	
2	0.40, 0.513	1.19, 10	1.13, 10	1.43, 10	120	68	100	
3	0.60, 0.769	1.19, 10	1.13, 10	1.43, 10	120	62	100	
4	0.20, 0.256	1.19, 10	1.70, 15	1.43, 10	120	92	100	
5	0.20, 0.256	1.19, 10	2.27, 20	1.43, 10	120	95	100	
6	0.20, 0.256	1.78, 15	2.27, 20	1.43, 10	60	90	100	
7	0.20, 0.256	2.38, 20	2.27, 20	1.43, 10	60	99	100	
9	0.20, 0.256	1.78, 15	1.70, 15	1.43, 10	60	93	100	
10	0.20, 0.256	2.38, 20	1.70, 15	1.43, 10	60	87	100	
11	0.20, 0.256	1.78, 15	1.70, 15	2.13, 15	60	93	100	
12	0.20, 0.256	1.78, 15	2.27, 20	2.13, 15	60	99	100	
13	0.20, 0.256	2.38, 20	2.27, 20	2.13, 15	30	97	100	
14	0.20, 0.256	1.78, 15	2.27, 20	2.86, 20	30	99	100	
15	**0.20, 0.256**	**2.38, 20**	**2.27, 20**	**2.86, 20**	**15**	**98**	**100**	
16	0.20, 0.256	2.38, 20	2.27, 20	2.86, 20	20	100	98	2
17	0.20, 0.256	2.38, 20	2.27, 20	2.86, 20	30	100	85	15

Table 3. Oxidative Bromination of Different Phenol Derivatives Using $[V^{IV}OTPP(CN)_4]$ (2) as the Catalyst

$$\text{phenols} \xrightarrow[\text{2 equiv. KBr, 2 equiv. } HClO_4, H_2O, \text{ rt}]{\text{0.00256 mol\% } \mathbf{2}, \text{ 2 equiv. 30\% } H_2O_2} \text{brominated phenols}$$

entry	substrate	time (min)	conv. (%)	TOF (s^{-1})	products	selectivity (%)
1.	phenol	15	97	42.0	4-bromophenol	55
					2-bromophenol	45
2.	4-methylphenol	15	98	42.5	2-bromo-4-methylphenol	100
3.	2-*iso*-propyl-5-methylphenol	15	95	41.2	2-bromo-3-methyl-6-*iso*-propylphenol	11
					4-bromo-3-methyl-6-*iso*-propylphenol	43
					2,4-dibromo-3-methyl-6-*iso*-propylphenol	46
4.	4-*tert*-butylphenol	15	99	42.9	2-bromo-4-*tert*-butylphenol	100
5.	2,4-dimethylphenol	15	100	43.3	2-bromo-4,6-*di*-methylphenol	100
6.	2,6-dimethylphenol	15	82	35.5	2,6-di-methyl-4-bromophenol	100
7.	2,4-di-*tert*-butylphenol	15	96	41.6	2,4-di-*tert*-butyl-6-bromophenol	100
8.	2-*tert*-butyl-4-methylphenol	15	95	41.2	2-bromo-4-methyl-6-*tert*-butylphenol	100
9.	4-bromophenol	15	96	41.6	2,4,-di-bromophenol	100
10.	2,4-dichlorophenol	15	85	36.8	2-bromo-4,6-di-chlorophenol	100
11.	4-methoxyphenol	15	100	43.3	2-bromo-4-methoxyphenol	76
					2,6-dibromo-4-methoxyphenol	24

complexes **1** and **2** are both axially compressed. Furthermore, we cannot observe any super hyperfine splitting from pyrrolic-N since the unpaired electron resides on a σ-non-bonding orbital pointing away from these N atoms, which are present in the equatorial (xy) plane.[34]

Catalytic Activity—Oxidative Bromination of Phenol Derivatives. Oxidative bromination of various phenol

Table 4. Oxidative Bromination of Different Phenol Derivatives Using [VOTPP(Br)$_4$] (1) as the Catalyst

$$\text{phenols} \xrightarrow[\text{2 equiv. KBr, 2 equiv. HClO}_4, \text{H}_2\text{O, rt}]{\text{0.00402 mol\% 1, 2 equiv. 30\% H}_2\text{O}_2} \text{brominated phenols}$$

entry	substrate	time (min)	conversion (%)	TOF (s⁻¹)	products	selectivity (%)
1.	phenol	15	94	26.0	4-bromophenol	58
					2-bromophenol	42
2.	4-methylphenol	15	95	26.3	2-bromo-4-methylphenol	100
3.	2-*iso*-propyl-5-methylphenol	15	93	25.7	2-bromo-3-methyl-6-*iso*-propylphenol	8
					4-bromo-3-methyl-6-*iso*-propylphenol	48
					2,4-dibromo-3-methyl-6-*iso*-propylphenol	44
4.	4-*tert*-butylphenol	15	97	26.8	2-bromo-4-*tert*-butylphenol	100
5.	2,4-dimethylphenol	15	99	27.4	2-bromo-4,6-di-methylphenol	100
6.	2,6-dimethylphenol	15	80	22.1	2,6-di-methyl-4-bromophenol	100
7.	2,4-di-*tert*-butylphenol	15	95	26.3	2,4-di-*tert*-butyl-6-bromophenol	100
8.	2-*tert*-butyl-4-methylphenol	15	94	26.0	2-bromo-4-methyl-6-*tert*-butylphenol	100
9.	4-bromophenol	15	93	25.7	2,4,-di-bromophenol	100
10.	2,4-dichlorophenol	15	82	22.7	2-bromo-4,6-di-chlorophenol	100
11.	4-methoxyphenol	15	99	27.4	2-bromo-4-methoxyphenol	80
					2,6-dibromo-4-methoxyphenol	20
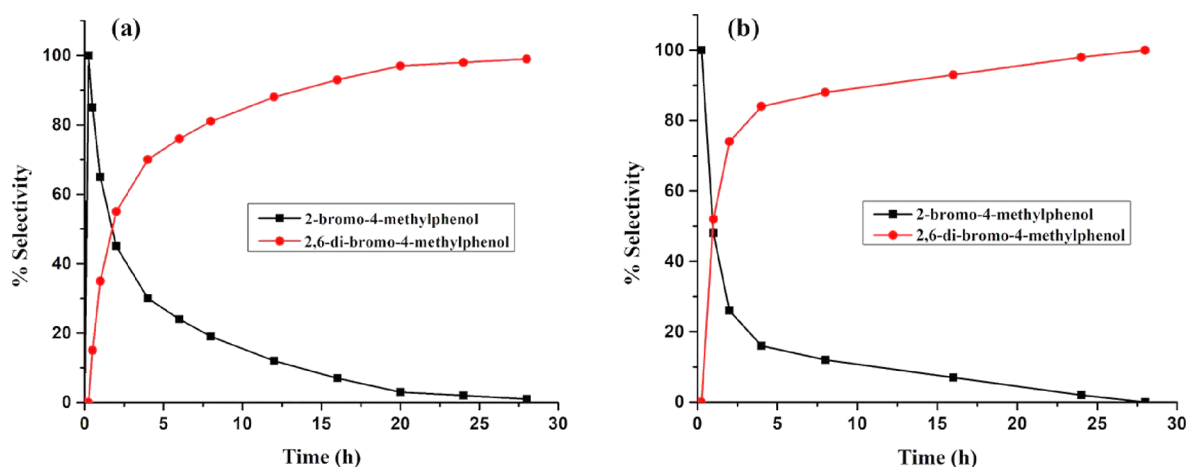
Figure 5. Time courses of the product selectivity change of the brominated product of 4-methylphenol using (a) catalyst **1** and (b) catalyst **2**.

derivatives was carried out considering complex **2** as a representative. Since the hydroxyl group at the phenyl ring is *o*- and *p*-directing, the bromination occurs on one or both of these positions depending on the situation. Considering 4-methylphenol as a representative, the following parameters were varied to optimize the reaction conditions for 10 mmol (1.08 g) of 4-methylphenol: (i) three different amounts of catalyst **2** (0.00020, 0.00040, and 0.00060 g), (ii) three different amounts of KBr (10, 20, and 30 mmol), (iii) three different amounts of oxidant 30% aqueous H$_2$O$_2$ (10, 20, and 30 mmol), and (iv) three different amounts of 70% aqueous HClO$_4$ (10, 20, and 30 mmol). Furthermore, reaction was carried out in water (20 mL) at room temperature. Table 2 presents the details of conversion under each specified condition. Mainly one product, i.e., 2-bromo-4-methylphenol, was formed at the optimized reaction conditions. However, the 100% conversion led to the formation of additional derivative *di*-bromo-4-methylphenol along with the initial product when the reaction time was extended. These products were confirmed by GC−MS (Figures S7 and S8).

The best-suited conditions for the maximum conversion of 10 mmol of 4-methylphenol (1.08 g) were found to be as follows: catalyst **2** (0.00020 g, 0.256 μmol), KBr (2.38 g, 20 mmol), 30% aqueous H$_2$O$_2$ (2.267 g, 20 mmol), 70% aqueous HClO$_4$ (2.87

g, 20 mmol, added in two equal portions of 1.43 g, each at interval of 5 min), and water (20 mL) (entry 15, Table 2). Notably, conversion reached 98% under these reaction conditions within 15 min with a TOF value of 42.5 s⁻¹, which is found to be very high as compared to any known vanadyl complex till date (Table S1).[16,27] There is no indication of the self bromination of **2** within this short period. This was further confirmed by the UV−visible spectrum (Figure 1) and MALDI-TOF mass spectrum (discussed in later sections) of the recovered complex after the catalytic reaction.

Oxidative bromination of other phenol derivatives (phenol, 4-*tert*-butylphenol, 2,4-dimethyl-phenol, 2,6-dimethylphenol, 2,4-di-*tert*-butylphenol, 2-*tert*-butyl-4-methyl-phenol, 4-bromophenol, 2,4-dichlorophenol, 4-methoxyphenol) (Table 3) was also carried out under similar reaction conditions as optimized for 4-methylphenol. Percentage conversion in most cases reaches above 95% except for 2,6-dimethylphenol (82%) and 2,4-dichlorophenol (85%). Generally, the monobromo product is obtained selectively, except in phenol and 4-methoxyphenol where the selectivities of the monobromo product are 55 and 76%, respectively. It was found that electron-donating groups enhance the reactivity of phenol, thereby resulting in relatively

higher yields and high turnover frequency (TOF) for electron-rich phenols.

Compared to **2**, complex **1** shows a bit lower conversion, but the selectivity trend of monobromo derivatives is the same (Table 4) as observed for **2**. The better performance of complex **2** compared to **1** is possibly due to better electron-withdrawing cyano groups and moderate nonplanarity.[35−39] Compared to the previously reported non-substituted vanadyl porphyrin $[V^{IV}OTPP]$ (TOF = 10.6−15.1 $s^{−1}$),[12] the catalytic activity of **1** (TOF = 22.1−27.4 $s^{−1}$) is found to be much better while that of **2** (TOF = 35.5−43.3 $s^{−1}$) is excellent.

To understand the conversion of a monobromo product to a dibromo analogue by extending time, we analyzed the product selectivity with an extended time period in the case of 4-methylphenol for both catalysts. It was observed that the % selectivity of 2,6-dibromo-4-methylphenol increases with the elapse of time and, after ca. 28 h, only 2,6-dibromo-4-methylphenol was observed in the reaction mixture (Figure 5). This is due to further bromination of the mono brominated product. This observation invigorated us to extend this study to another mono-substituted phenol (i.e., 4-methoxyphenol) where the possibility of further electrophilic (Br^+) substitution exists and the same trend is found (Figure S9). In the case of phenol, the initially formed 2-bromophenol as well as 4-bromophenol both converted to 2,4-dibromophenol (Figure S10).

Reactivity of Complexes 1 and 2 with Brominating Reagents in the Absence of a Brominating Substrate. As observed earlier during the oxidative bromination, complex $[V^{IV}OTTP]$ used as the catalyst underwent self-bromination in the absence of a substrate and gave β-octabrominated complex $[V^{IV}OTTP(Br)_8]$.[12] Under similar optimized reaction conditions, i.e., when a mixture of 2.5 mmol of KBr, 2.5 mmol of H_2O_2, and 1.0 mmol of $HClO_4$ in 3 mL of water was used and a solution of 0.05 mmol of complex **1** in 2 mL of dichloromethane was added, the stirring of reaction for 36 h at room temperature also gave complex $[V^{IV}OTTP(Br)_8]$ (Scheme 4), which was

Scheme 4. Self-Catalytic Oxidative Bromination Behavior of Complex 1 to Give Octabromo Derivative $[V^{IV}OTTP(Br)_8]$
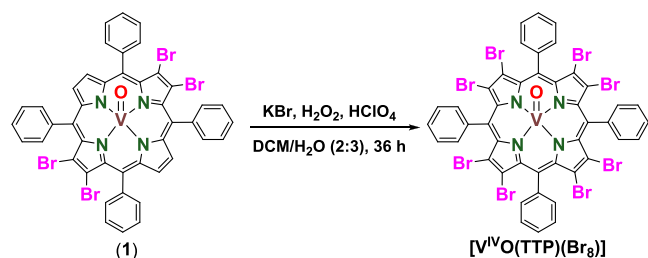
confirmed by UV−vis spectroscopy [UV−vis ($CHCl_3$) λ_{max} (nm): 362, 464, 590, 628] (Figure 6) as well as MALDI-TOF mass spectrometry [m/z: found 1310.04 $[M]^+$ (calcd. 1310.44) (Figure S11). Interestingly, complex **2** showed no observable change in the UV−vis spectrum under similar reaction conditions, indicating no bromination at the unsubstituted β-position. This is possibly due to the strong electron-withdrawing nature of tetracyano substituents that oppose the electrophilic (Br^+) substitution at the β-position.

Catalytic Activity—Epoxidation of Olefins. As epoxidation of olefins was already reported for catalyst **1**,[29] the catalytic potential of **2** was also established here for the
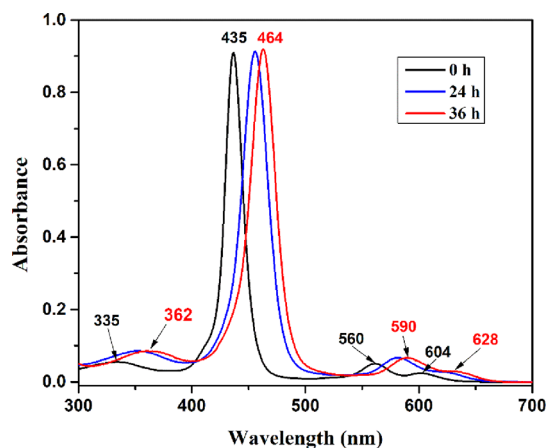
Figure 6. UV−vis spectral change during the self-catalytic reaction of catalyst **1**.

epoxidation of various olefins. We have chosen styrene as a representative alkene, and the following parameters were varied to optimize the reaction conditions: for 5 mmol (0.52 g) of styrene: (i) three different amounts of the catalyst (0.0005, 0.001, and 0.0015 g), (ii) three different amounts of the oxidant 30% aqueous H_2O_2 (10, 15, and 20 mmol), (iii) three different amounts of $NaHCO_3$ (promoter) (1.5, 2.0, and 2.5 mmol) at various compositions of solvents ($MeCN/H_2O$) (5:0, 3:1, 2:1, 3:2, and 4:3). Furthermore, the reaction was carried out at two temperatures (i.e., 50 and 60 °C). Table 5 presents the details of conversion under each specified condition (optimization parameters). The best-suited reaction conditions were concluded to be as follows (entry 8, Table 5): styrene 0.52 g, 5 mmol; catalyst **2** 0.0005 g, 0.641 μmol; oxidant H_2O_2 2.26 g, 20 mmol; promotor $NaHCO_3$ 0.168 g, 2.0 mmol, in a 3:2 $MeCN$:H_2O mixture (v/v) at 60 °C. Under these conditions, a maximum of 92% conversion of styrene to styrene epoxide selectively was achieved within 1 h of reaction time.
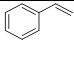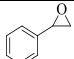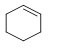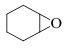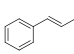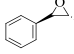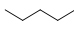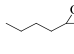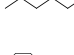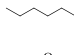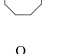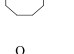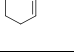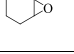
Under the above optimized reaction conditions, epoxidation of other alkenes was also tested (Table 6) and corresponding epoxides were obtained selectively with good conversion. Controlled experiments (i.e., in the absence of catalyst and/or promoter $NaHCO_3$) were also performed, and the results demonstrate that the oxidant is essential to achieving good catalytic conversion while the promoter is essential to achieving selectivity toward the formation of epoxide. It is observed that, in the absence of catalyst **2**, conversion is only 40% under the optimized reaction conditions, while in the absence of $NaHCO_3$ (promoter), conversion was found to be 39% under the same conditions. In the absence of both catalyst **2** and $NaHCO_3$ (promoter), the conversion was limited only to 15%.

Recyclability of Catalysts during Oxidative Bromination and Epoxidation. Catalysts **1** and **2** were recovered after the first cycle of bromination reaction using column chromatography, as detailed in the Experimental Section. The efficiency of both recovered catalysts was examined again for the oxidative bromination of 4-methylphenol under conditions similar to those used for the first cycle. Recycled **1** exhibited 94% conversion of 4-methylphenol with a TOF of 26.0 $s^{−1}$, while recycled **2** exhibited a conversion of 96% and a TOF of 41.6 $s^{−1}$. The minor loss in catalytic efficiency can be explained by the fact that the recovery process of a very small amount of catalyst, especially in homogeneous catalysis, is not 100% efficient and inevitably leads to a small loss of the catalyst. Catalyst

Table 5. Oxidation of Styrene (0.52 g, 5 mmol) Using $[V^{IV}OTPP(CN)_4]$ (2) as the Catalyst in 1 h Reaction Time under Different Reaction Conditions

entry	catalyst (mg, μmol)	H_2O_2 (g, mmol)	$NaHCO_3$ (g, mmol)	$MeCN/H_2O$	temp. (°C)	% conversion	selectivity
1.	0.5, 0.641	1.13, 10	0.168, 2	3:2	60	80	100
2.	1.0, 1.28	1.13, 10	0.168, 2	3:2	60	83	100
3.	1.5, 1.92	1.13, 10	0.168, 2	3:2	60	69	100
4.	0.5, 0.641	1.70, 15	0.168, 2	3:2	60	88	100
5.	0.5, 0.641	2.26, 15	0.126, 1.5	3:2	60	67	100
6.	0.5, 0.641	2.26, 20	0.126, 1.5	3:2	60	78	100
7.	0.5, 0.641	2.26, 20	0.210, 2.5	3:2	60	61	100
8.	**0.5, 0.641**	**2.26, 20**	**0.168, 2**	**3:2**	**60**	**92**	**100**
9.	0.5, 0.641	2.26, 20	0.168, 2	2:1	60	76	100
10.	0.5, 0.641	2.26, 20	0.168, 2	4:3	60	53	100
11.	0.5, 0.641	2.26, 20	0.168, 2	3:1	60	65	100
12.	0.5, 0.641	2.26, 20	0.168, 2	5:0	60	49	100
13.	0.5, 0.641	2.26, 20	0.168, 2	3:2	50	75	100
14.		2.26, 20	0.168, 2	3:2	60	40	100
15.		2.26, 20		3:2	60	15	100
16.	0.5, 0.641	2.26, 20		3:2	60	39	100

Table 6. Oxidation of Various Olefins Using Catalysts 2 under Optimized Reaction Conditions with 100% Selectivity for the Epoxide Formation

$$\text{olefin} \xrightarrow[\text{0.4 equiv. } NaHCO_3, \text{ } MeCN/H_2O, \text{ 60 °C}]{\text{0.013 mol\% 2, 4 equiv. 30\% } H_2O_2} \text{epoxide}$$

entry	substrate	product	conversion (%)	TOF (s^{-1})
1			92	2.00
2			98	2.12
3			93	2.01
4			92	2.00
5			94	2.03
6			96	2.08
7			91	1.97

recyclability was repeated four times, and only a small decrease in conversion was noticed. Even in the fourth cycle, catalysts **1** and **2** showed 85 and 86% conversion, respectively (Figure 7).

The recyclability of catalysts **2** was also tested four times for the epoxidation of styrene under similar optimized reaction conditions as fixed for epoxidation, and again, only a minor decrease in efficiency (Figure 8) was noted.

Recovery of Catalysts after Catalytic Reaction and Their Characterization. The UV−vis spectra of the recovered catalysts slightly differ (Figure 9) from the respective fresh catalyst. The MALDI-TOF mass spectra of these recovered catalysts show the formation of a stable intermediate $[V^VO-(OH)TPP(Br)_4]$ (**1a**) [(m/z) found: 1011.247, $[M]^-$ calc: 1011.81)] and $[V^VO(OH)TPP(CN)_4]$ (**2a**) [(m/z): 795.167, $[M-H]^-$ calc: 795.15], i.e., oxido-hydroxidovanadium(V) analogues of complexes **1** and **2** (Figures S12 and S13). This
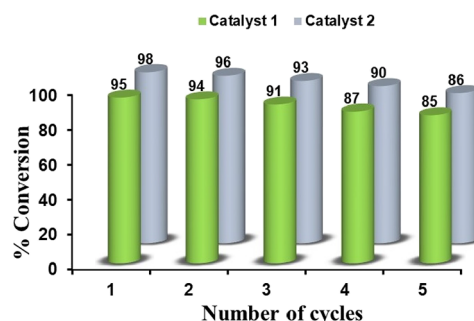
Figure 7. Bar diagram showing catalytic recyclability along with % conversion at every cycle of catalytic reaction (bromination of 4-methylphenol) using **1** (green) and **2** (gray).
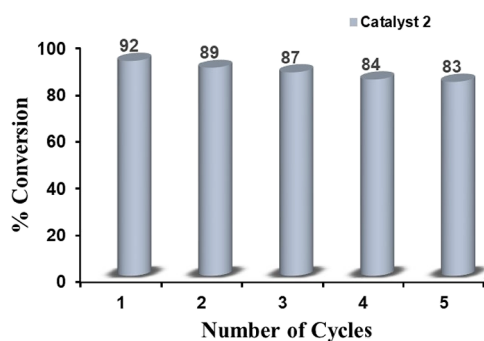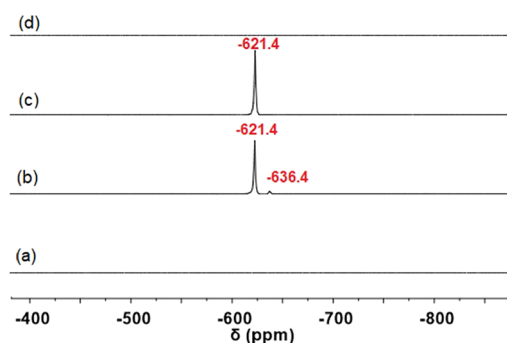
Figure 8. Bar diagram showing catalytic recyclability along with % conversion at every cycle of catalytic reaction (epoxidation of styrene) using **2**.

Figure 10. ^{51}V NMR spectra of $[V^{IV}OTPP(CN)_4]$ (**2**) (6.4 μmol) in DMSO-d_6 (a) in the presence of a fresh sample, (b) after adding 0.44 mmol of 30% aq. H_2O_2 and 0.37 mmol of $NaHCO_3$ to (a), (c) after heating the solution in (b) for 1 h at 60 °C, and (d) after adding excess of styrene to (c) and heating at 60 °C for 10 min.

observation further suggests that catalysts change their structures after catalytic oxidative bromination reaction.

Catalyst **2** after epoxidation of styrene was also recovered and purified through column chromatography, and its UV−vis spectrum and MALDI-TOF mass spectrum were recorded. While the mass spectrum matches well with the sample recovered after bromination reaction, the UV−vis spectrum showed one extra band at ca. 270 nm (Figure S14), which is possibly the presence of a trace amount of styrene epoxide as styrene epoxide exhibits a UV band at ca. 260 nm (Figure S15).

Reactivity of $[V^{IV}OTPP(CN)_4]$ (2) in DMSO-d_6—A ^{51}V NMR Study and Possible Catalytic Mechanism. In order to understand the mechanistic pathway for the epoxidation of organic substrates, we performed a ^{51}V NMR study of complex **2** under different conditions. The ^{51}V NMR spectra of **2** were recorded as (i) fresh sample dissolved in DMSO-d_6 (Figure 10a), (ii) after adding H_2O_2 and $NaHCO_3$ to (a) (Figure 10b), (iii) sample (b) after heating for 1 h at 60 °C (Figure 10c), and (iv) after adding excess styrene to (c) (Figure 10d). Thus, as expected pure paramagnetic complex **2** dissolved in DMSO-d_6 gave no peak in ^{51}V NMR. However, upon addition of 0.44 mmol of 30% aqueous H_2O_2 and 0.37 mmol of $NaHCO_3$, two NMR signals were observed at −621.4 and −636.4 ppm with an intensity ratio of 9.5:0.5. Based on the UV−vis and MALDI-TOF spectral studies of the recovered catalyst (see previous section), the former signal may be assigned due to the generation of $[V^VO(OH)TPP(CN)_4]$ while the weak signal at

−636.4 ppm might be due to oxidoperoxidovanadium(V) species.[40,41] Heating the reaction mixture for 1 h at 60 °C, the minor signal at −636.4 ppm disappeared, possibly due to breaking of the peroxide species to a relatively better stable intermediate $[V^VO(OH)TPP(CN)_4]$. The signal at −621.4 ppm completely disappeared upon addition of excess of styrene to the above solution. The styrene containing the above solution was also subjected to MALDI-TOF mass spectrometry, and the resulting spectrum (Figure S16) shows the appearance of a new but weak signal due to original complex **2** along with the signal due to $[V^VO(OH)TPP(CN)_4]$. These two observations hint toward the further reaction of $[V^VO(OH)TPP(CN)_4]$ with styrene and converting it back to the original complex to some extent. Thus, it is reasonable to propose that during styrene epoxidation, catalyst **2** passes through highly unstable intermediate oxidoperoxidovanadium(V) to a relatively better stable oxidohydroxidovanadium(V) intermediate. The oxidohydroxidovanadium(V) complex upon further reaction with H_2O_2 in the presence of $NaHCO_3$ again forms the highly unstable oxidoperoxidovanadium(V) species,[42] and the reaction continues.

The oxidative bromination only partly follows the reaction mechanism generally followed by vanadium complexes (Scheme 1). Complex **2** reacts with H_2O_2 to give the corresponding oxidoperoxidovanadium(V) intermediate, which in the presence
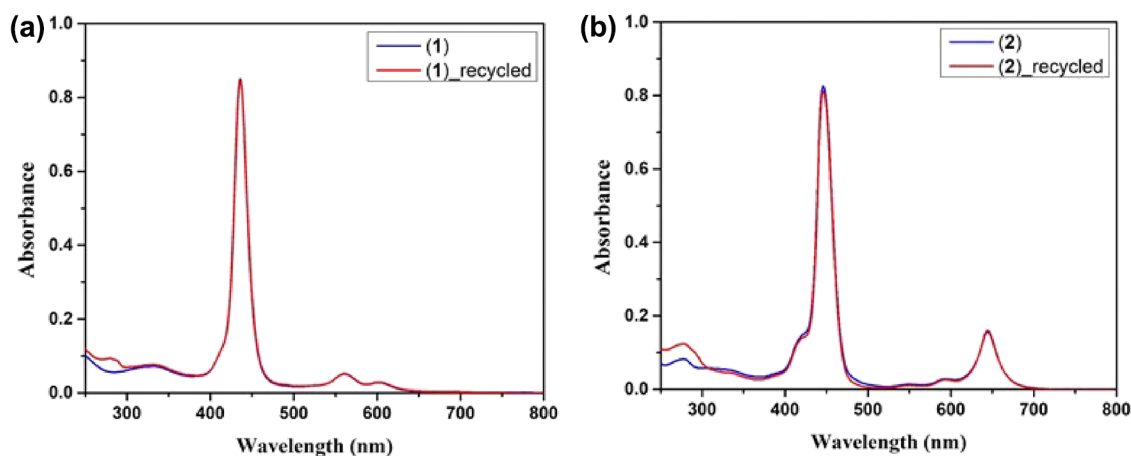
Figure 9. (a) UV−vis spectra of **1** before (blue) and after (red) catalytic reaction and (b) UV−vis spectra of **2** before (blue) and after (red) catalytic reaction.

of H_3O^+ (i.e., aqueous $HClO_4$) possibly changes to oxidohydroperoxidovanadium(V) porphyrin. Both species are possibly highly unstable, the latter of which catalyzes the oxidation of Br^- to HOBr; a brominating reagent and a catalyst are converted to a better stable $[V^VO(OH)TPP(CN)_4]$. Like epoxidation, the reaction continues in the presence of H_2O_2 and $HClO_4$.

CONCLUSIONS

A simplified method was developed to synthesize a highly electron-deficient β-tetracyano-*meso*-tetraphenylporphyrin vanadyl complex, $[V^{IV}OTPP(CN)_4]$ (**2**) from β-tetrabromo-substituted vanadyl porphyrin $[V^{IV}OTPP(Br)_4]$ (**1**) by nucleophilic substitution reaction. The catalytic potential of complexes **1** and **2** was tested for the oxidative bromination of phenol and its derivatives. Catalyst **2**, being more electron deficient, was found as the best catalyst for the oxidative bromination reaction having a TOF value of 43.3 s^{-1}, the highest TOF found for any catalyst till date. Although catalysts **1** and **2** are homogeneous catalysts, they are recyclable and their recyclability was checked up to four cycles. Catalyst **2** was also utilized for the selective epoxidation of olefins, and conversions were good to excellent. As evidenced by UV−vis, MALDI-TOF mass, and ^{51}V NMR studies, both catalysts are recyclable and both catalytic reactions pass through the corresponding $[V^VO(OH)TPP(Br)_4]$ or $[V^VO(OH)TPP(CN)_4]$ intermediate.

EXPERIMENTAL SECTION

Materials. $VOSO_4$, N-bromosuccinimide (HiMedia, India), CuCN (SD Fine Chemicals, India), various alkenes (Alfa Aesar, India), 30% aqueous H_2O_2, silica gel (100−200 mesh) (Rankem, India), and HPLC-grade DMF (SRL) were used as received. Tetrabutylammonium hexafluorophosphate (TBAPF$_6$) (Merck) was recrystallized two times from hot ethanol before use. H_2TPPBr_4 was prepared from H_2TPP using recrystallized N-bromosuccinimide.[9] Dry CH_2Cl_2 used in cyclic voltammetry analysis was distilled twice after drying over phosphorus pentoxide (P_2O_5) and from calcium hydride (CaH_2) for the third time.

Instrumentation. Elemental analysis was carried out using an Elementar vario EL II instrument. Mid-IR range IR spectra were recorded using a Perkin-Elmer spectrometer as KBr pellet. UV−vis spectra were recorded using an Agilent Cary 100 spectrophotometer. Cyclic voltammetric measurements were performed on a CHI 620E instrument, using a three-electrode assembly that consisted of Ag/AgCl as the reference electrode, Pt disk as the working electrode, and Pt wire as the counter electrode. All electrochemical measurements were carried out in triple-distilled CH_2Cl_2 using TBAF$_6$ as the supporting electrolyte, Pt as the working electrode, Ag/AgCl as the reference electrode, and Pt wire as the counter electrode at 298 K. Using HABA as a matrix, MALDI-TOF spectra were recorded on a Bruker UltrafleXtreme-TN MALDI-TOF mass spectrometer. SII EXSTAR 6300 was used to obtain thermogravimetric analysis with a heating rate of 10 °C/min under a normal aerial atmosphere using aluminum powder as reference. EPR spectra were recorded in EMXmicro A200-9.5/12/S/W, BRUKER BIOSPIN, and simulated by WINEPR SimFonia. Reaction products obtained from the catalytic reaction were identified using a Shimadzu 2010 Plus gas chromatograph endowed with an Rtx-1 capillary column (30 m × 0.25 mm × 0.25 μm) and an FID detector. The product identities were confirmed using a

Perkin-Elmer GC−MS (Clarus 500). The percent (%) conversion of the substrate and the selectivity of the products were calculated from the GC data using the formulae

$$\%\text{conversion of substrate} = 100 - \frac{\text{peak area of a substrate}}{\text{total area of substrate + products}} \times 100$$

$$\%\text{selectivity of a product} = \frac{\text{peak area of a product}}{\text{total area of products}} \times 100$$

Synthesis of $[V^{IV}OTPP(Br)_4]$, 1. Complex **1** was synthesized by the method reported by us previously.[29] Yield 85% (271 mg, 0.272 mmol). UV−vis (CH_2Cl_2): λ_{max} (nm) (log ε): 335 (3.98), 435 (5.28), 560 (4.00), 604 (3.80). MALDI-TOF-MS (m/z): found 995.99 $[M]^+$, calcd. 995.24. Anal. calcd. for $C_{44}H_{24}Br_4N_4OV$: C, 53.10; H, 2.43; N, 5.63. Found C, 52.99; H, 2.46; N, 5.22.

Synthesis of $[V^{IV}OTPP(CN)_4]$, 2. *Method A.* Complex **1** (100 mg, 0.1005 mmol) was dissolved in 15 mL of quinoline, and CuCN (900 mg, 10.05 mmol, ca. 100 equiv.) was added. The reaction mixture was stirred for 10 min and then heated with stirring at 190 °C for 3 h under an argon atmosphere. The reaction mixture was cooled to ambient temperature and filtered using a G-4 crucible. The filtrate was diluted with chloroform (30 mL) and washed with 10 M HCl solution (3 × 25 mL) followed by water (3 × 25 mL). After drying the chloroform layer with sodium sulfate, the solvent was removed by a rotary evaporator. The crude product was dissolved in chloroform and purified over silica (100−200 mesh) using chloroform as the eluent. The last and major band of three fractions was collected and identified as **2**. Complex **2** was obtained in pure form by rotatory evaporation of the solvent. Yield 32% (25 mg, 0.0321 mmol). UV−vis (CH_2Cl_2): λ_{max} (nm) (log ε): 443 (5.31), 578 (3.81), 625 (4.67). MALDI-TOF-MS (m/z): found 779.53 $[M]^+$, calcd. 779.15. Anal. calcd. for $C_{48}H_{24}N_8OV$: C, 73.94; H, 3.10; N, 14.37. Found: C, 73.75; H, 3.01; N, 14.22.

Method B. Alternatively, **2** was also prepared as follows: ligand 2,3,12,13-tetracyano-5,10,15,20-tetraphenylporphyrin (300 mg, 0.420 mmol) was dissolved in DMF (75 mL). A large excess of $VOSO_4$ hydrate (1027.5 mg, 6.3 mmol) was added to it, and the mixture was stirred for 10 min and then refluxed for 30 h under an argon atmosphere. The reaction mixture was cooled to room temperature and distilled water (150 mL) was added, and the product mixture was allowed to settle as precipitate. It was then filtered using the G-4 crucible and dried under vacuum for 8 h. The crude product was re-dissolved in $CHCl_3$ and purified over silica (100−200) mesh using chloroform as the eluent. Compound **2** was obtained in pure form by rota-evaporating the eluent in 55% yield (212 mg, 0.273 mmol). UV−vis (CH_2Cl_2): λmax (nm) (log ε): 437 (5.31), 635 (4.67). MALDI-TOF-MS (m/z): found 779.53 $[M]^+$, calcd 779.15. Anal. calcd. for $C_{48}H_{24}N_8OV$: C, 73.94; H, 3.10; N, 14.37. Found: C, 73.79; H, 2.96; N, 14.20.

Catalytic Activity—Oxidative Bromination of Phenol Derivatives. In a typical reaction, 4-methylphenol, a representative (1.08 g, 10 mmol), KBr (2.38 g, 20 mmol), 30% aqueous H_2O_2 (2.26 g, 20 mmol), and water (20 mL) were taken in a 50 mL reaction flask. Complex **2** (0.00020 g, 0.262 μmol) and $HClO_4$ (1.43 g, 10 mmol) were added, and the mixture was stirred at room temperature. An additional 10 mmol of $HClO_4$ was added after 5 min. After 15 min, the reaction mixture was extracted with hexane and the hexane layer was

injected (ca. 0.25 μL) into the gas chromatograph. The products were finally analyzed by GC−MS and identified by the electronic library available. Similar reactions were performed using 0.402 μmol of catalyst **1**.

Recovery and Reuse of Catalysts. After completing the first cycle of the catalytic reaction as mentioned above in five different batches for both substrates (i.e., styrene and phenol), CHCl₃ was added to each reaction mixture and washed with distilled water (3 × 10 mL) and organic layer separated. Both catalysts were recovered by silica column chromatography using CHCl₃:hexane (3:7, v/v) for **1** and CHCl₃ for **2** as eluent. Their identities were confirmed by UV−vis and MALDI-TOF mass spectrometry (Figures S12 and S13). The recovered catalysts were used for the next cycle of catalytic reaction.

■ ASSOCIATED CONTENT

ⓈⒾ Supporting Information

The Supporting Information is available free of charge at https://pubs.acs.org/doi/10.1021/acsomega.2c06638.

> Characterization data, NMR spectra, MALDI-TOF mass spectra, TGA, catalytic information, TOF (h^{-1}) values for oxidative bromination of thymol/terpenes with different catalysts known in the literature (PDF)

■ AUTHOR INFORMATION

Corresponding Authors

Mannar R. Maurya − *Department of Chemistry, Indian Institute of Technology Roorkee, Roorkee 247667, India;* ⓞ orcid.org/0000-0001-9977-6287; Email: m.maurya@cy.iitr.ac.in

Muniappan Sankar − *Department of Chemistry, Indian Institute of Technology Roorkee, Roorkee 247667, India;* ⓞ orcid.org/0000-0001-6667-3759; Email: m.sankar@cy.iitr.ac.in

Authors

Ved Prakash − *Department of Chemistry, Indian Institute of Technology Roorkee, Roorkee 247667, India*

Tawseef Ahmad Dar − *Department of Chemistry, Indian Institute of Technology Roorkee, Roorkee 247667, India*

Complete contact information is available at:
https://pubs.acs.org/10.1021/acsomega.2c06638

Notes

The authors declare no competing financial interest.

■ ACKNOWLEDGMENTS

■ REFERENCES

(1) Leblanc, C.; Vilter, H.; Fournier, J. B.; Delage, L.; Potin, P.; Rebuffet, E.; Michel, G.; Solari, P. L.; Feiters, M. C.; Czjzek, M. Vanadium haloperoxidases: From the discovery 30 years ago to X-ray crystallographic and V K-edge absorption spectroscopic studies. *Coord. Chem. Rev.* **2015**, *301-302*, 134−146.

(2) (a)) Butler, A.; Baldwin, A. H. Vanadium bromoperoxidase and functional mimics. *Struct. Bonding* **1997**, *89*, 109−132. (b)) Plass, W.; Bangesh, M.; Nica, S.; Buchholz, A. Model Studies of Vanadium-Dependent Haloperoxidation: Structural and Functional Lessons, Synthetic and Computational Models of Supramolecular Interactions and the Formation of Peroxo Species. *ACS Symp. Ser.* **2007**, *974*, 163−177.

(3) (a)) Clague, M. J.; Keder, N. L.; Butler, A. Biomimics of vanadium bromoperoxidase: Vanadium(V)-Schiff base catalyzed oxidation of bromide by hydrogen peroxide. *Inorg. Chem.* **1993**, *32*, 4754. (b)) Butler, A. Mechanistic considerations of the vanadium haloperoxidases. *Coord. Chem. Rev.* **1999**, *187*, 17−35.

(4) Nica, S.; Pohlmann, A.; Plass, W. Vanadium(V) Oxoperoxo Complexes with Side Chain Substituted *N*-Salicylidenehydrazides: Modeling Supramolecular Interactions inVanadium Haloperoxidases. *Eur. J. Inorg. Chem.* **2005**, 2032−2036.

(5) Wischang, D.; Hartung, J.; Hahn, T.; Ulber, R.; Stumpf, T.; Fecher-Trost, C. Vanadate(v)-dependent bromoperoxidase immobilized on magnetic beads as reusable catalyst for oxidative bromination. *Green Chem.* **2011**, *13*, 102−108.

(6) Maurya, M. R. Probing the synthetic protocols and coordination chemistry of oxido-, dioxido-, oxidoperoxido-vanadium and related complexes of higher nuclearity. *Coord. Chem. Rev.* **2019**, *383*, 43−81.

(7) Tótaro, R. M.; Williams, P. A. M.; Apella, M. C.; Blesa, M. A.; Baran, E. J. Bromination of phenol red mediated by vanadium (V) peroxo complexes at pH 6.5. *J. Chem. Soc. Dalton Trans.* **2000**, 4403−4406.

(8) Chang, C. K.; Kuo, M. S. Reaction of Iron(III) Porphyrins and Iodosoxylene; The Active Oxene Complex of Cytochrome P-450. *J. Am. Chem. Soc.* **1979**, *101*, 3413−3415.

(9) Vicente, M.; Smith, K. Syntheses and Functionalizations of Porphyrin Macrocycles. *Curr. Org. Synth.* **2014**, *11*, 3−28.

(10) Suslick, K. S.; Bhyrappa, P.; Chou, J. H.; Kosal, M. E.; Nakagaki, S.; Smithenry, D. W.; Wilson, S. R. Microporous Porphyrin Solids. *Acc. Chem. Res.* **2005**, *38*, 283−291.

(11) Suslick, K. S.; Rakow, N. A.; Kosal, M. E.; Chou, J. H. The materials chemistry of porphyrins and metalloporphyrins. *J. Porphyrins Phthalocyanines* **2000**, *04*, 407−413.

(12) Maurya, M. R.; Prakash, V.; Avecilla, F.; Sankar, M. Selective Bromination of β-Positions of Porphyrin by Self-Catalytic Behaviour of VOTPP: Facile Synthesis, Electrochemical Redox Properties and Catalytic Application. *Eur. J. Inorg. Chem.* **2021**, 1685−1694.

(13) Weissermel, K.; Arpe, H. J.; *Industrial Organic Chemistry*, VCH , 1997, DOI: 10.1002/9783527616688.

(14) Rao, A. S.; Paknikar, S. K.; Kirtane, J. G. Recent advances in the preparation and synthetic applications of oxiranes. *Tetrahedron* **1983**, *39*, 2323−2367.

(15) Yamazaki, S. Metalloporphyrins and related metallomacrocycles as electrocatalysts for use in polymer electrolyte fuel cells and water electrolyzers. *Coord. Chem. Rev.* **2018**, *373*, 148−166.

(16) Dar, T. A.; Uprety, B.; Sankar, M.; Maurya, M. R. Robust and electron deficient oxidovanadium(IV) porphyrin catalysts for selective epoxidation and oxidative bromination reactions in aqueous media. *Green Chem.* **2019**, *21*, 1757−1768.

(17) Han, Y.; Fang, H.; Jing, H.; Sun, H.; Lei, H.; Lai, W.; Cao, R. Singly versus Doubly Reduced Nickel Porphyrins for Proton Reduction: Experimental and Theoretical Evidence for a Homolytic Hydrogen-Evolution Reaction. *Angew. Chem., Int. Ed.* **2016**, *55*, 5457−5462.

(18) Hardison, R. C. A brief history of hemoglobins: Plant, animal, protist, and bacteria. *Proc. Natl. Acad. Sci. U. S. A.* **1996**, *93*, 5675−5679.

(19) Mauzerall, D.Porphyrins, Chlorophyll, and Photosynthesis. In *Photosynthesis I*; Springer Berlin Heidelberg: Berlin, Heidelberg, 1977, 117−124.

(20) Feierabend, J.; Dehne, S. Fate of the porphyrin cofactors during the light-dependent turnover of catalase and of the photosystem II reaction-center protein D1 in mature rye leaves. *Planta* **1996**, *198*, 413−422.

(21) Birel, Ö.; Nadeem, S.; Duman, H. Porphyrin-Based Dye-Sensitized Solar Cells (DSSCs): a Review. *J. Fluoresc.* **2017**, *27*, 1075−1085.

(22) Ethirajan, M.; Chen, Y.; Joshi, P.; Pandey, R. K. The role of porphyrin chemistry in tumor imaging and photodynamic therapy. *Chem. Soc. Rev.* **2011**, *40*, 340−362.

(23) Ding, Y.; Zhu, W.-H.; Xie, Y. Development of Ion Chemosensors Based on Porphyrin Analogues. *Chem. Rev.* **2017**, *117*, 2203−2256.

(24) Barona-Castaño, J.; Carmona-Vargas, C.; Brocksom, T.; de Oliveira, K. Porphyrins as Catalysts in Scalable Organic Reactions. *Molecules* **2016**, *21*, 310−336.

(25) Senge, M. O.; Fazekas, M.; Notaras, E. G. A.; Blau, W. J.; Zawadzka, M.; Locos, O. B.; Ni Mhuircheartaigh, E. M. Nonlinear optical properties of porphyrins. *Adv. Mater.* **2007**, *19*, 2737−2774.

(26) Bhyrappa, P.; Sankar, M.; Varghese, B. Mixed Substituted Porphyrins: Structural and Electrochemical Redox Properties. *Inorg. Chem.* **2006**, *45*, 4136−4149.

(27) Kumar, R.; Chaudhary, N.; Sankar, M.; Maurya, M. R. Electron deficient nonplanar β-octachlorovanadylporphyrin as a highly efficient and selective epoxidation catalyst for olefins. *Dalton Trans.* **2015**, *44*, 17720−17729.

(28) Kumar, P. K.; Bhyrappa, P.; Varghese, B. An improved protocol for the synthesis of antipodal β-tetrabromo-tetraphenylporphyrin and the crystal structure of its Zn(II) complex. *Tetrahedron Lett.* **2003**, *44*, 4849−4851.

(29) Dar, T. A.; Tomar, R.; Mian, R. M.; Sankar, M.; Maurya, M. R. Vanadyl β-tetrabromoporphyrin: synthesis, crystal structure and its use as an efficient and selective catalyst for olefin epoxidation in aqueous medium. *RSC Adv.* **2019**, *9*, 10405−10413.

(30) Kumar, R.; Saxena, A.; Sankar, M. Mixed β-bromo/cyano tetrasubstituted-meso-tetraphenylporphyrin Cu(II) complexes: Synthesis and electrochemical studies. *J. Porphyrins Phthalocyanines* **2016**, *20*, 1420−1425.

(31) Kadish, K. M.; Morrison, M. M. Substituent effects on the redox reactions of tetraphenylporphyrins. *Bioinorg. Chem.* **1977**, *7*, 107−115.

(32) Kadish, K. M. The Electrochemistry of Metalloporphyrins in Nonaqueous Media. *Prog. Inorg. Chem.* **2007**, *34*, 435−605.

(33) Ghosh, S. K.; Patra, R.; Rath, S. P. Axial Ligand Coordination in Sterically Strained Vanadyl Porphyrins: Synthesis, Structure, and Properties. *Inorg. Chem.* **2008**, *47*, 9848−9856.

(34) Smith, T. S., II; LoBrutto, R.; Pecoraro, V. L. Paramagnetic spectroscopy of vanadyl complexes and its applications to biological systems. *Coord. Chem. Rev.* **2002**, *228*, 1−18.

(35) Langeslay, R. R.; Kaphan, D. M.; Marshall, C. L.; Stair, P. C.; Sattelberger, A. P.; Delferro, M. Catalytic Applications of Vanadium: A Mechanistic Perspective. *Chem. Rev.* **2019**, *119*, 2128−2191.

(36) Sabuzi, F.; Pomarico, G.; Floris, B.; Valentini, F.; Galloni, P.; Conte, V. Sustainable bromination of organic compounds: A critical review. *Coord. Chem. Rev.* **2019**, *385*, 100−136.

(37) Pessoa, J. C.; Correia, I. Salan vs. salen metal complexes in catalysis and medicinal applications: Virtues and pitfalls. *Coord. Chem. Rev.* **2019**, *388*, 227−247.

(38) Galloni, P.; Mancini, M.; Floris, B.; Conte, V. A sustainable two-phase procedure for V-catalyzed toluene oxidative bromination with H_2O_2-KBr. *Dalton Trans.* **2013**, *42*, 11963−11970.

(39) McLauchlan, C. C.; Murakami, H. A.; Wallace, C. A.; Crans, D. C. Coordination environment changes of the vanadium in vanadium-dependent haloperoxidase enzymes. *J. Inorg. Biochem.* **2018**, *186*, 267−279.

(40) (a) Balcells, D.; Maseras, F.; Ujaque, G. Computational Rationalization of the Dependence of the Enantioselectivity on the Nature of the Catalyst in the Vanadium-Catalyzed Oxidation of Sulfides by Hydrogen Peroxide. *J. Am. Chem. Soc.* **2005**, *127*, 3624−3634. (b) Kravitz, J. Y.; Pecoraro, V. L.; Carlson, H. A. Quantum Mechanics/Molecular Mechanics Calculations of the Vanadium Dependent Chloroperoxidase. *J. Chem. Theory Comput.* **2005**, *1*, 1265−1274. (c) Schneider, C. J.; Penner-Hanh, J. E.; Pecoraro, V. L. Elucidating the Protonation Site of Vanadium Peroxide Complexes and the Implications for Biomimetic Catalysis. *J. Am. Chem. Soc.* **2008**, *130*, 2712−2713.

(41) Maurya, M. R.; Haldar, C.; Kumar, A.; Kuznetsov, M.; Avecilla, F.; Costa Pessoa, J. Vanadium complexes having $[VO]^{2+}$, $[VO]^{3+}$ and $[VO_2]^+$ cores with hydrazones of 2,6-diformyl-4-methylphenol: synthesis, characterization, reactivity, and catalytic potential. *Dalton Trans.* **2013**, *42*, 11941−11962.

(42) (a)) Maiti, S. K.; Dinda, S.; Banerjee, S.; Mukherjee, A. K.; Bharracharyya, R. Oxidoperoxidotungsten(VI) Complexes with Secondary Hydroxamic Acids: Synthesis, Structure and Catalytic Uses in Highly Efficient, Selective and Ecologically Benign Oxidation of Olefins, Alcohols, Sulfides and Amines with H_2O_2 as a Terminal Oxidant. *Eur. J. Inorg. Chem.* **2008**, *2008*, 2038. (b)) Bagherzadeh, M.; Aminia, M.; Parastar, H.; Jalali-Heravi, M.; Ellern, A.; Woo, L. K. *Inorg. Chem. Commun.* **2012**, *20*, 86−89. (c)) Lane, B. S.; Vogt, M.; DeRose, V. J.; Burgess, K. Manganese-Catalyzed Epoxidations of Alkenes in Bicarbonate Solutions. *J. Am. Chem. Soc.* **2002**, *124*, 11946−11954. (d)) Richardson, D. E.; Yao, H.; Frank, K. M.; Bennett, D. A. Equilibria, Kinetics, and Mechanism in the Bicarbonate Activation of Hydrogen Peroxide: Oxidation of Sulfides by Peroxymonocarbonate. *J. Am. Chem. Soc.* **2000**, *122*, 1729−1739.